Projected lung area using dynamic X-ray (DXR) with a flat-panel detector system and automated tracking in patients with chronic obstructive pulmonary disease (COPD)

日野, 卓也

European Journal of Radiology 157 (2022) 110546

Contents lists available at ScienceDirect

European Journal of Radiology

journal homepage: www.elsevier.com/locate/ejrad

Projected lung area using dynamic X-ray (DXR) with a flat-panel detector system and automated tracking in patients with chronic obstructive pulmonary disease (COPD)

Takuya Hino [a,*], Akinori Tsunomori [b], Takenori Fukumoto [b], Akinori Hata [c], Tomoyuki Hida [d], Yoshitake Yamada [e], Masako Ueyama [f], Takeshi Kamitani [d], Mizuki Nishino [a], Atsuko Kurosaki [g], Masahiro Jinzaki [e], Kousei Ishigami [d], Hiroshi Honda [d], Tsutomu Yoneyama [b], Sumiya Nagatsuka [b], Shoji Kudoh [h], Hiroto Hatabu [a]

[a] Center for Pulmonary Functional Imaging, Department of Radiology, Brigham and Women's Hospital, Harvard Medical School, 75 Francis St., Boston, MA, USA
[b] R&D Promotion Division, Healthcare Business Headquarters, KONICA MINOLTA, INC., 2970 Ishikawa-machi, Hachioji-shi, Tokyo, Japan
[c] Department of Radiology, Graduate School of Medicine, Osaka University, 2-2 Yamadaoka, Suita, Osaka, Japan
[d] Department of Clinical Radiology, Graduate School of Medical Sciences, Kyushu University, 3-1-1 Maidashi, Higashi-ku, Fukuoka, Fukuoka, Japan
[e] Department of Diagnostic Radiology, Keio University School of Medicine, 35 Shinanomachi, Shinjuku-ku, Tokyo, Japan
[f] Department of Health Care, Fukujuji Hospital, Japan Anti-Tuberculosis Association, 3-1-24 Matsuyama, Kiyose, Tokyo, Japan
[g] Department of Diagnostic Radiology, Fukujuji Hospital, Japan Anti-Tuberculosis Association, 3-1-24 Matsuyama, Kiyose, Tokyo, Japan
[h] Japan Anti-Tuberculosis Association, 1-3-12 Kanda-Misakicho, Chiyoda-ku, Tokyo, Japan

ARTICLE INFO

Keywords:
Dynamic X-ray
Chest radiograph
Pulmonary function
COPD
Projected lung area

ABSTRACT

Objectives: To assess the association of projected lung area (PLA) measured by DXR with demographic data, pulmonary function, and COPD severity, and to generate PLA over time curves using automated tracking.
Methods: This retrospective study recruited healthy volunteers and COPD patients. Participants were classified into three groups: normal, COPD mild and COPD severe. PLA was calculated from the manually traced bilateral lung contours. PLA over time curves were produced using automated tracking, which was used to calculate slope and intercept by approximate line during forced expiration. The correlation of PLA, difference of PLA between end-inspiration and end-expiration (ΔPLA), slope, and intercept with demographic data and pulmonary function tests were investigated. The difference of PLA, ΔPLA, intercept, and slope among three groups were also evaluated.
Results: This study enrolled 45 healthy volunteers and 32 COPD patients. COPD severe group had larger PLA in both lungs at tidal/forced end-inspiration/expiration, smaller slope, and larger intercept than normal group ($p < 0.001$). PLA was correlated with % forced expiratory volume in one second (%FEV_1) (r_s from −0.42 to −0.31, $p \leq 0.01$). ΔPLA in forced breathing showed moderate correlation with vital capacity (VC) ($r_s = 0.58$, $p < 0.001$), while ΔPLA in tidal breathing showed moderate correlation with %FEV_1 ($r_s = -0.52$, $p < 0.001$) as well as mild correlation with tidal volume ($r_s = 0.24$, $p = 0.032$). Intercept was slightly underestimated compared with manually contoured PLA ($p < 0.001$).
Conclusion: COPD patients had larger PLA than healthy volunteers. PLA and ΔPLA in tidal breathing showed mild to moderate correlation with %FEV_1.

Abbreviations: COPD, chronic obstructive pulmonary disease; DXR, dynamic X-ray; ΔPLA, the difference of PLA between end-inspiration and end-expiration in tidal or forced breathing; FEV_1, forced expiratory volume percent in one second; FEV_1%VC, forced expiratory volume percent in one second divided by forced vital capacity; GOLD, global initiative for chronic obstructive lung disease; %FEV_1, percent predicted forced expiratory volume in one second; %VC, percent predicted vital capacity; PLA, projected lung area; PFT, pulmonary function test; rs, Spearman's rank correlation coefficient; TV, tidal volume; VC, vital capacity.

Peer review under responsibility of If file "editor conflict of interest statement" is present in S0, please extract the information and add it as a footnote (star) to the relevant author. The sentence should read (and be amended accordingly): Given his/her role as EditorinChief/Associate Editor/Section Editor <NAME of Editor> had no involvement in the peerreview of this article and has no access to information regarding its peerreview..

* Corresponding author at: Center for Pulmonary Functional Imaging, Department of Radiology, Brigham and Women's Hospital and Harvard Medical School, 75 Francis Street, Boston, MA 02215, USA.
E-mail address: hino.takuya.372@m.kyushu-u.ac.jp (T. Hino).

https://doi.org/10.1016/j.ejrad.2022.110546
Received 25 February 2022; Received in revised form 20 September 2022; Accepted 24 September 2022
Available online 29 September 2022

1. Introduction

Progressive airflow limitation and airway inflammation characterizes chronic obstructive pulmonary disease (COPD) [1]. COPD has multiple different aspects of pathology, pathophysiology and clinical presentations [1–3]. Comorbidity and mortality of COPD remain important issues [3,4]. The main abnormality in COPD is the destruction of pulmonary parenchyma with loss of lung elastic recoil, peripheral muscle atrophy and overload ventilation [5,6]. Airflow limitation and subsequent air trapping can contribute to hyperinflation of both lungs [5–7].

Recently, dynamic X-ray (DXR) using a flat-panel detector with a large field of view was introduced in clinical setting. DXR can generate dynamic sequential images of the thorax with high-temporal resolution up to 15 frames per second [8,9]. DXR is a much simpler examination compared to CT or MRI. The previous studies have reported utility of DXR in the analysis and evaluation of diaphragmatic motions in COPD patients [10,11]. Previous study has shown the association between pulmonary function tests and projected lung area (PLA) measured from DXR images in healthy subjects [12].

We hypothesized that COPD patients has larger PLA than normal subjects on the basis of hyperinflation of lungs induced by COPD. It is also anticipated that the difference of PLA in tidal or forced breathing between end-inspiration and end-expiration (ΔPLA) is larger in COPD patients due to compensatory breathing. The aim of the current study is to assess the association of PLA with demographic data, pulmonary function and COPD severity, and to visualize automated PLA over time using curved graph.

2. Materials and methods

2.1. Population selection

This retrospective study was approved by research ethics committee. Written informed consent was obtained from all the participants. COPD patients were recruited from June 2009 to August 2011, while healthy volunteers from May 2013 to February 2014. Common inclusion criteria for all the participants are as follows [10,11]: (1) $\geq$ 20 years old adults with informed consent; (2) schedule for conventional chest radiograph; (3) comprehension and ability to follow instructions for tidal or forced breathing; (4) no status of pregnancy, potential pregnancy, or lactation.

The additional inclusion criteria for COPD patients are as follows [10,11]: (5) clinical diagnosis of COPD based on clinical course, symptoms, CT, and pulmonary function test (PFT) after the use of bronchodilator; (6) former or current smokers; (7) no evidence of other respiratory disease, whereas those for healthy volunteers: (5) normal vital capacity (VC) and forced expiratory volume percent in one second (FEV_1) according to the GOLD criteria; (6) never smokers; (7) no past medical history of respiratory diseases.

All the COPD subjects were classified into four grades according to global initiative for chronic obstructive lung disease (GOLD) based on spirometry with corresponding percent predicted forced expiratory volume in one second (%FEV_1) [3]. This study defined COPD GOLD 1/2 as mild, and GOLD 3/4 as severe.

2.2. Data acquisition of DXR image and PFTs

DXR of the posteroanterior view was performed in standing position using a prototype X-ray system (Konica Minolta Inc., Tokyo, Japan) composed of a flat-panel detector (PaxScan 4030CB, Varian Medical Systems Inc., Salt Lake City, UT, USA) and a pulsed X-ray generator (DHF-155HII with Cineradiography option, Hitachi Medical Corporation, Tokyo, Japan). Healthy volunteers took several tidal breaths and following one forced breath, while COPD patients took tidal breaths and forced breath separately. Conditions for DXR examination were almost the same as the previous reports [8–12]: tube voltage, 100 kV; tube current, 50 mA; pulse duration of pulsed X-ray, 1.6 ms; source-to-image distance, 2 m; additional filter, 0.5 mm Al + 0.1 mm Cu; the pixel size, 388 × 388 μm; the matrix size, 1024 × 768; the overall image area, 40 × 30 cm; the exposure time, 10–15 s. The additional filter was used to remove soft X-rays. The dynamic image data, captured at 15 frames/s except for one case with 7.5 frames/s, were synchronized with the pulsed X-ray, which could reduce the entrance surface dose to the subjects within the tolerant range from 0.3 to 1.0 mGy.

DXR data were analyzed using prototype software (Konica Minolta Inc., Tokyo, Japan) installed in an independent workstation (Operating system: Windows 7 Professional 64-bit Service Pack 1; Microsoft, Redmond WA; CPU: Intel® CoreTM i5-6500, 3.20 GHz; random access memory, 16 GB). Nine-year-experienced radiologist manually contoured the border of bilateral lung fields with the exclusion of both heart and mediastinum. Then PLA and ΔPLA were automatically measured. DXR examination include several phases of tidal breaths; PLA of all the tidal respiratory phase was measured and calculated for the better data reliability. The averaged PLAs in several tidal respiratory phases were taken in this study. The graph of averaged pixel values and time was referenced to identify particular respiratory phase [9,11].

Bilateral lung fields of DXR images were also contoured with full automation by software invented by Konica Minolta Inc. The temporal change of automatically tracked PLA could be visualized by curved graph. Straight line fitting of curved graph during forced expiration was performed to obtain intercept and the absolute value of slope, defined as "slope" in this study. Intercept is expected to approximate manually contoured PLA, while slope to correlate with FEV_1.

All participants underwent both PFTs and DXR on the same day. A pulmonary function instrument with computer processing (DISCOM-21 FX, Chest MI Co, Tokyo, Japan) was used for PFT. Parameters of PFTs were following the guideline of American Thoracic Society [13]: tidal volume (TV), VC, percent predicted vital capacity (%VC), FEV_1, forced expiratory volume percent in one second divided by forced vital capacity (FEV_1%VC), and %FEV_1.

2.3. Statistical analysis

The difference of demographic data and pulmonary function between normal, COPD mild and COPD severe groups were examined with one-way analysis of variance. The difference of sex ratio was studied with Fisher's exact test. The correlation of PLA, slope, and intercept with each parameter as well as that between ΔPLA in tidal respiration and TV, between ΔPLA in forced respiration and VC, and between intercept and manually contoured PLA were assessed with Spearman's rank correlation coefficient. Multiple linear regression analysis was also performed for adjusting confound factors; PLA was set as dependent variables, and potentially associated parameters with PLA, including age, sex, height, and %FEV_1 as independent variables. Multiple comparison of PLA, ΔPLA, slope, and intercept among the three groups was performed using one-way analysis of variance with Holm-Bonferroni correction. The difference and correlation between manually and automatically tracked PLA were assessed with paired *t*-test and Pearson's correlation coefficient. The error of manually and automatically tracked was analyzed with Bland-Altman plot. The degree of coincidence between two methods were quantified with intraclass correlation coefficient (ICC).

Statistical analyses were conducted with EZR (Saitama Medical Center, Jichi Medical University, Saitama, Japan). EZR is a graphical user interface for R4.0.3 (R Foundation for Statistical Computing, Vienna, Austria) [14]. More precisely, it is a modified version of R commander designed to add statistical functions frequently used in biostatistics. A two-sided P values $\leq$ 0.050 were considered statistically significant.

3. Results

3.1. Inclusion/exclusion criteria

Flow chart of criteria is shown in Fig. 1. Four healthy subjects were excluded because of incomplete dataset of DXR (n = 3) and suspiciously inadequate nourishment (n = 1), while eleven COPD patients were excluded due to the following reasons: incomplete dataset of DXR (n = 9) and notable image noises (n = 2). Finally, a total of 45 healthy volunteers and 32 COPD patients were enrolled in this study. Healthy volunteers served as normal group. Fifteen COPD patients were allocated with COPD mild group. Whereas eighteen COPD patients were allocated with severe group.

3.2. Demographic data and pulmonary function

Demographic data and pulmonary function categorized by normal, COPD mild and COPD severe groups are shown in Table 1. Age, sex, PFTs were different among three groups with statistical significance. Representative cases are shown in normal (Fig. 2), COPD mild (Fig. 3), and COPD severe group (Fig. 4). The PLA over time curves were successfully generated using the automated tracking.

3.3. PLA/ΔPLA versus pulmonary function

The scatter plots of PLA in both lungs and $\%FEV_1$ showed that the correlation was mild to moderate in tidal inspiration/expiration and forced inspiration/expiration with r_s ranging from −0.42 to −0.31 ($p \leq 0.006$) (Fig. 5). The statistically significant correlation between ΔPLA in forced breathing and VC was observed ($r_s = 0.58$, $p < 0.001$) (Fig. 6). Whereas ΔPLA in tidal breathing showed mild correlation with TV ($r_s = 0.24$; $p = 0.032$) (Fig. 6).

3.4. Comparison of PLA among normal, COPD mild and COPD severe groups

Table 2 showed PLA and difference of PLA between end-inspiration and end-expiration (ΔPLA) in tidal/forced respiratory phases in both lungs with multiple comparison by one-way analysis of variance with Holm-Bonferroni correction. PLAs were significantly different between normal and COPD Severe groups in both tidal inspiration/expiration and forced inspiration/expiration in both lungs ($p \leq 0.002$). PLA in forced expiratory phase was also different with statistical significance between COPD mild and COPD severe groups in the left lung ($p < 0.001$). Similar results were obtained with PLA of right and left lungs (Table S1). ΔPLA in tidal breathing was lower in normal subjects than COPD patients ($p < 0.001$), while ΔPLA in forced breathing was higher in normal group than in COPD severe group ($p = 0.013$).

Spearman's correlation coefficients of PLA with demographic data and PFTs in the right lung (Table S2a), left lung (Table S2b) and both lungs (Tables 3a and 3b) were shown. Sex, height, BMI, $FEV_1\%VC$, and $\%FEV_1$ showed mild to moderate correlation with PLA. The absolute value of correlation coefficient between PLA and $\%FEV_1$ was relatively higher, with r_s ranging from −0.42 to −0.31 ($p \leq 0.006$). ΔPLA in tidal breathing also showed moderate correlation with $\%FEV_1$ ($r_s = -0.52$, $p < 0.001$). Multiple linear regression analysis demonstrated that height and $\%FEV_1$ were significant factors accounting for PLA (Table S3).

3.5. Slope and intercept calculated by automated tracking of PLA

Intercept and slope were statistically different among the three groups ($p = 0.001$) (Table 2). Intercept were higher in COPD patients compared with healthy volunteers. Slope showed mild positive correlation with FEV_1 ($r_s = 0.35$, $p < 0.001$) (Table 4). Both slope and intercept showed positive correlation with VC (slope, $r_s = 0.46$, $p < 0.001$; intercept, $r_s = 0.39$, $p < 0.001$) (Table 4).

3.6. The quantification of error between manually and automatically tracked PLA

Automatically contoured PLA showed significant correlation with manually contoured PLA ($r = 0.96$, $p < 0.001$). Bland-Altman plot between manually and automatically contoured PLA was summarized in Figure S1. Automatically tracked PLA was smaller in value than manually contoured PLA ($p < 0.001$), which was regarded as fixed error. Bias (SD) calculated by Bland-Altman plot was −39.18 (20.07) as well as

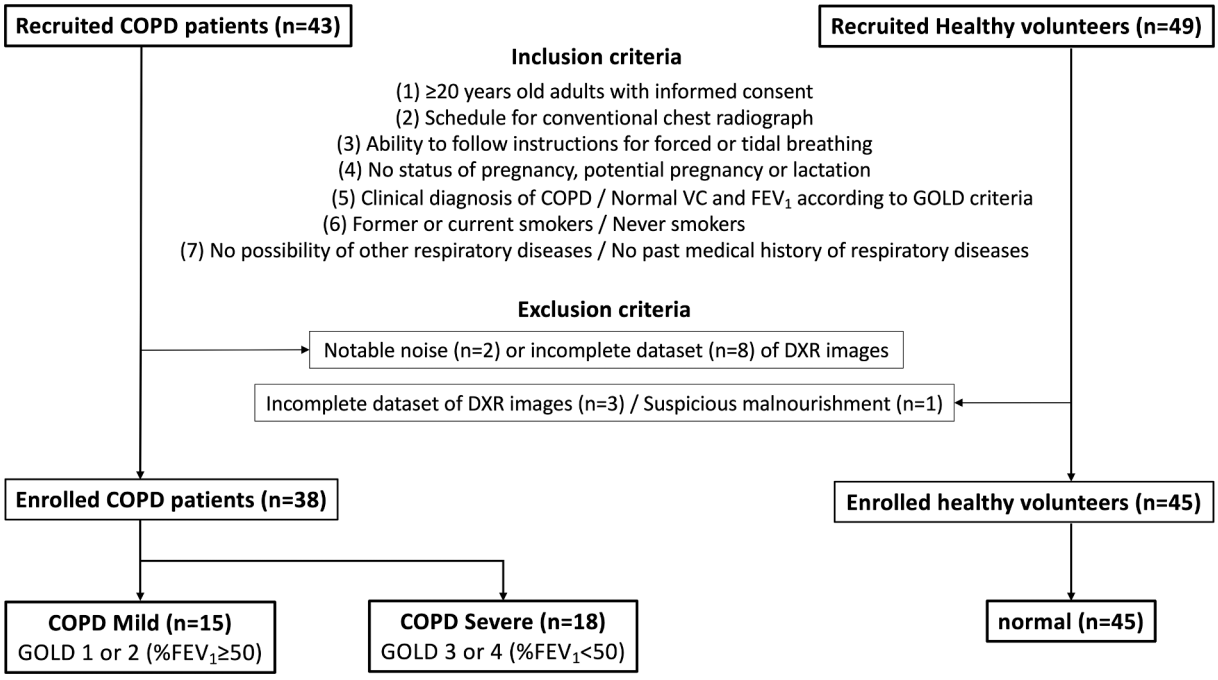

Fig. 1. Flow chart of inclusion and exclusion criteria. DXR, dynamic X-ray, $\%FEV_1$ percent predicted forced expiratory volume in one second; %VC, percent predicted vital capacity; PFT, pulmonary function test.

Table 1
Demographic data and pulmonary function tests among Normal, COPD mild, and COPD severe groups.

	Normal (n = 45)		COPD mild (n = 15)		COPD severe (n = 17)		
Variables	Mean ± SD [range]		Mean ± SD [range]		Mean ± SD [range]		P value
Demographic data							
Age (years)	54.5 ± 9.8	[36–72]	74.3 ± 10.0	[48–85]	68.6 ± 9.1	[54–85]	<0.001
Sex, Female/Male	26 / 19		2 / 13		2 / 15		<0.001
Height (cm)	162.2 ± 9.5	[146.1–183.7]	163.6 ± 5.6	[150.0–171.0]	163.5 ± 6.9	[150.0–176.0]	0.785
Weight (kg)	59.0 ± 10.3	[37.0–78.0]	58.1 ± 6.2	[46.0–67.0]	56.2 ± 14.5	[42.0–94.0]	0.671
BMI (kg/m^2)	22.3 ± 2.9	[15.1–31.1]	21.8 ± 2.3	[16.3–24.2]	20.9 ± 4.7	[16.5–34.5]	0.328
Smoking History	Never		Current or former		Current or former		
GOLD, 1/2/3/4	0 / 0 / 0 / 0		4 / 11 / 0 / 0		0 / 0 / 14 / 3		
PFTs							
TV (L)	0.76 ± 0.36	[0.34–1.76]	1.12 ± 0.48	[0.39–2.30]	0.88 ± 0.29	[0.54–1.67]	0.006
VC (L)	3.34 ± 0.88	[2.11–5.70]	3.14 ± 0.58	[2.35–4.34]	2.52 ± 0.70	[1.49–4.03]	0.002
%VC	110.2 ± 14.7	[92.1–159.6]	103.6 ± 17.9	[78.2–140.0]	79.2 ± 17.9	[44.6–111.3]	<0.001
FEV_1 (L)	2.70 ± 0.74	[1.58–4.72]	1.72 ± 0.33	[1.08–2.41]	0.99 ± 0.29	[0.52–1.60]	<0.001
FEV_1%VC	82.2 ± 6.2	[70.5–97.0]	57.5 ± 6.4	[45.8–68.9]	41.6 ± 4.5	[34.6–48.3]	<0.001
%FEV_1	106.5 ± 14.4	[80.6–163.9]	69.5 ± 12.9	[52.4–97.9]	36.7 ± 8.6	[16.3–47.1]	<0.001

BMI, body mass index; FEV_1, forced expiratory volume in one second; FEV_1%VC, forced expiratory volume percent in one second divided by forced vital capacity; GOLD, global initiative for chronic obstructive lung disease; %FEV_1, percent predicted forced expiratory volume percent in one second; %VC, percent predicted vital capacity; VC, vital capacity; TV, tidal volume.

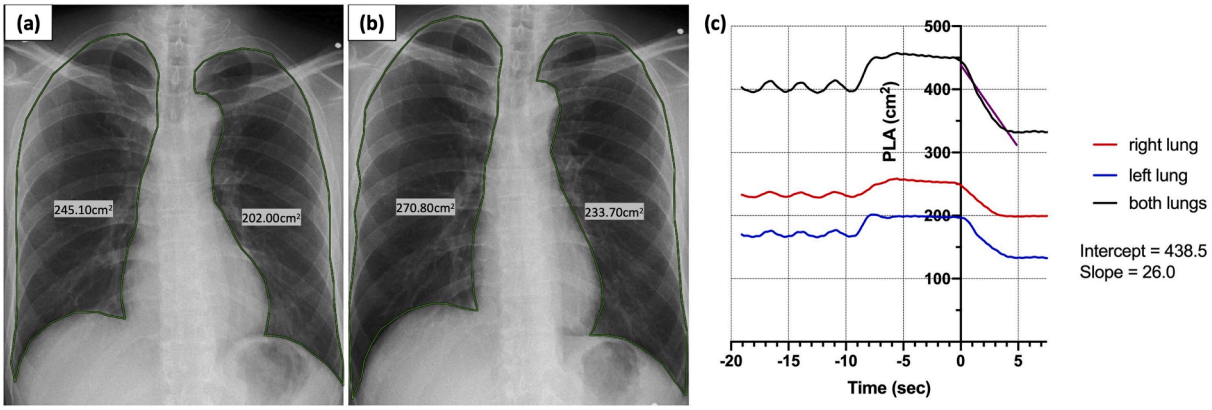

Fig. 2. 50-year-old male subject of normal group with FEV_1%VC 95.1 and %FEV_1 102.7. PLA of (a) tidal inspiratory phase and (b) forced inspiratory phase. (c) curve graph of the temporal change of PLA by automated tracking. Approximate straight line during forced expiration is colored purple. FEV_1%VC, forced expiratory volume percent in one second divided by forced vital capacity; PLA, projected lung area; %FEV_1 percent predicted forced expiratory volume in one second.

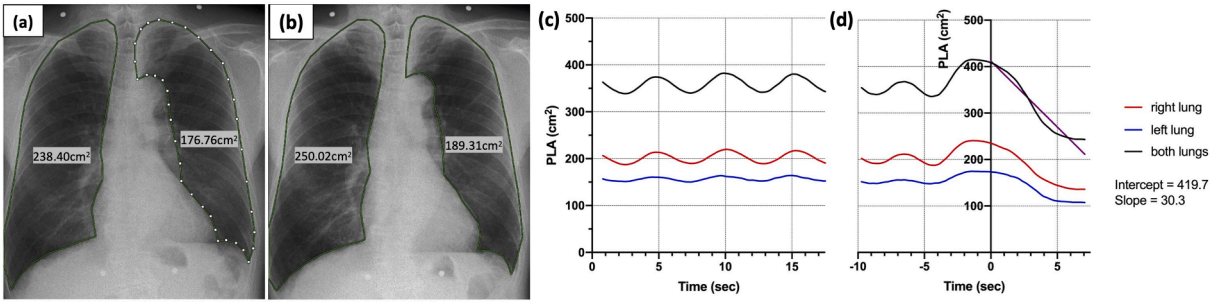

Fig. 3. 79-year-old male of COPD mild group with FEV_1%VC 53.1 and %FEV_1 72.6. PLA of (a) tidal inspiratory phase and (b) forced inspiratory phase. Image (a) describes manually located white dots in the left lung field, which was used for automatic calculation of left PLA. Curve graphs describe the temporal change of PLA by automated tracking in (c) tidal and (d) forced respiration. Approximate straight line during forced expiration is colored purple. FEV_1%VC, forced expiratory volume percent in one second divided by forced vital capacity; PLA, projected lung area; %FEV_1 percent predicted forced expiratory volume in one second.

limit of agreement from −78.52 to 0.16. Bland-Altman plot also suggested proportional error. ICC between the two methods was 0.822, considered "almost perfect" agreement.

4. Discussion

DXR with high temporal resolution help to extract images in particular phase, especially in tidal respiration. COPD groups had relatively larger PLA than normal group. The PLA versus time curves were successfully generated using the automated tracking, which generated the graphs simulating the spirometry. Intercept showed very strong correlation with manually contoured PLA ($r_s = 0.95$, $p < 0.001$) with a tendency of slight underestimation. This study indicated the possibility to quantify hyperinflation and visualization in COPD patients.

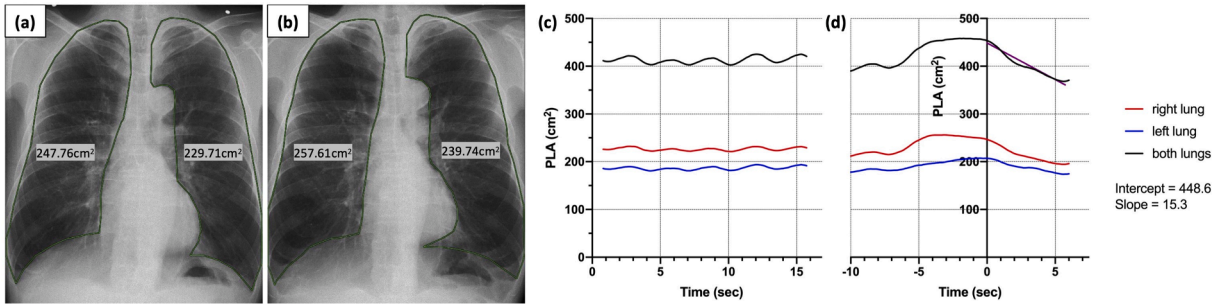

Fig. 4. 58-year-old male of COPD severe group with FEV_1%VC 35.6 and %FEV_1 30.5 PLA of (a) tidal inspiratory phase and (b) forced inspiratory phase. Curve graphs describe the temporal change of PLA by automated tracking in (c) tidal and (d) forced respiration. Approximate straight line during forced expiration is colored purple. FEV_1%, forced expiratory volume percent in one second divided by forced vital capacity; PLA, projected lung area; %FEV_1 percent predicted forced expiratory volume in one second.

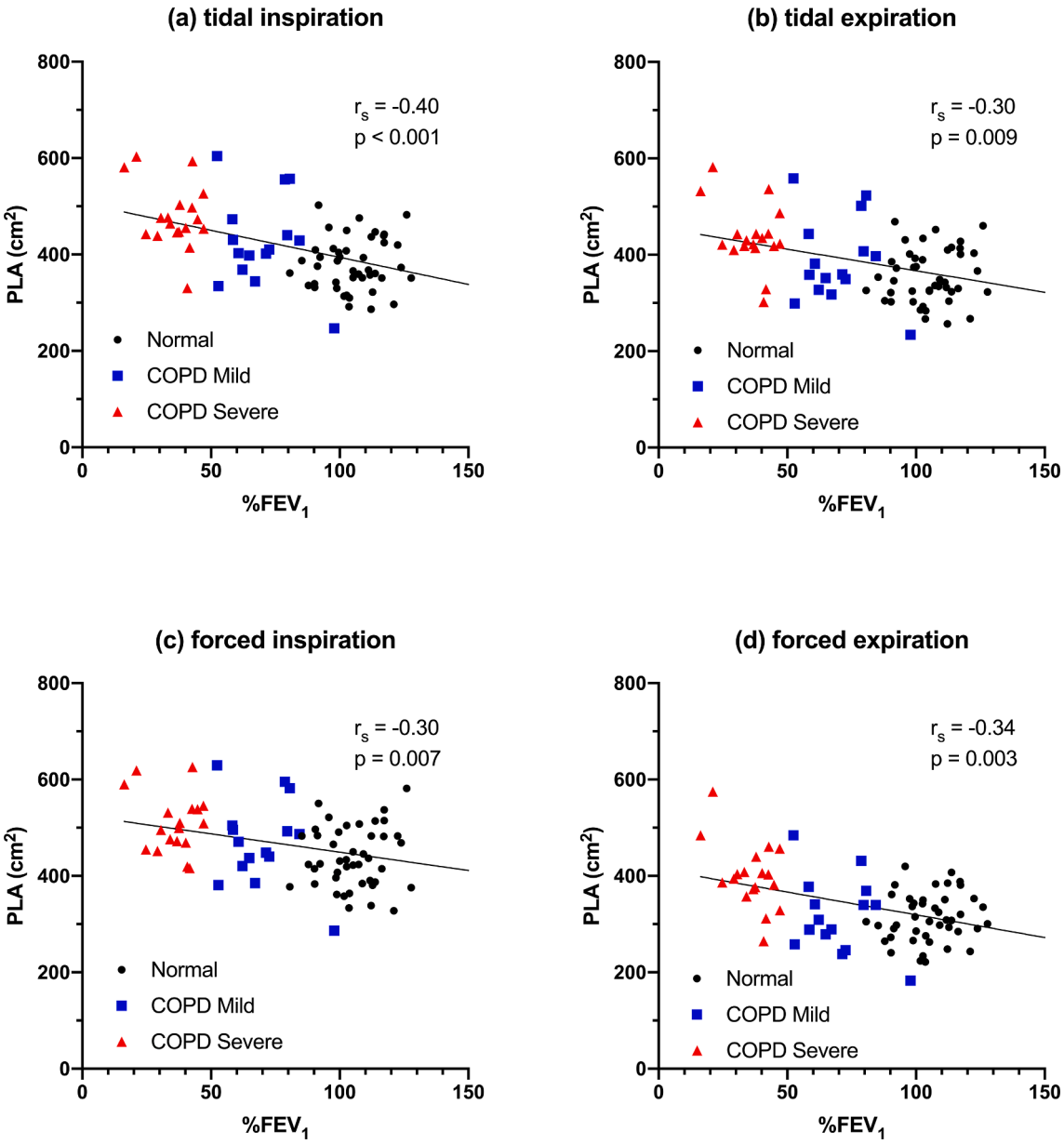

Fig. 5. The scatter plots of the association between PLA in both lungs and %FEV_1 in (a) tidal inspiratory, (b) tidal expiratory, (c) forced inspiratory, and (d) forced expiratory phases. The scatter plots visualize every case of normal (black dot), COPD mild (blue square), COPD severe (red triangle) groups with approximate line, showing mild to moderate correlation by Spearman's correlation coefficient with statistical significance. PLA, projected lung area; %FEV_1 percent predicted forced expiratory volume in one second.

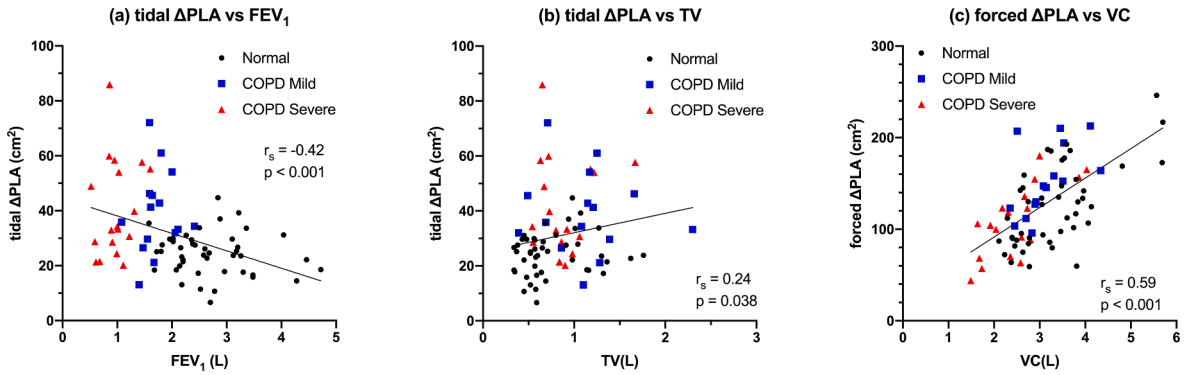

Fig. 6. The scatter plots of (a) %FEV_1 versus tidal ΔPLA, (b) TV versus tidal ΔPLA, (c) VC versus forced ΔPLA. Mild to moderate correlation by Spearman's rank correlation coefficient was confirmed. %FEV_1 percent predicted forced expiratory volume in one second; ΔPLA, difference of PLA between end-inspiration and end-expiration; TV, tidal volume; VC, vital capacity.

Table 2
PLA and ΔPLA in inspiratory and expiratory phases in both lungs.

	PLA, Mean ± SD (cm^2)			P values			
	Normal (n = 45) (1)	COPD mild (n = 15) (2)	COPD severe (n = 17) (3)	all†	1 vs 2‡	2 vs 3§	1 vs 3‖
PLA							
tidal inspiration	382.2 ± 55.4	426.5 ± 92.9	481.3 ± 67.8	<0.001**	0.046**	0.046**	<0.001**
tidal expiration	357.9 ± 57.1	387.2 ± 88.1	439.3 ± 68.4	<0.001**	0.142	0.060	<0.001**
tidal ΔPLA	24.4 ± 7.8	39.3 ± 15.3	42.0 ± 17.8	<0.001**	<0.001**	0.525	<0.001**
forced inspiration	440.7 ± 64.0	470.5 ± 88.7	512.3 ± 61.2	0.002**	0.182	0.182	0.001**
forced expiration	314.9 ± 50.6	318.3 ± 77.8	401.5 ± 71.2	<0.001**	0.853	<0.001**	<0.001**
forced ΔPLA	125.8 ± 44.5	152.2 ± 38.9	110.7 ± 39.6	0.003**	0.080	0.022*	0.217
Slope (cm^2/*sec*)	24.1 ± 8.9	26.1 ± 8.6	16.7 ± 5.6	0.003**	0.407	0.006**	0.006**
Intercept (cm^2)	392.8 ± 52.3	426.6 ± 77.2	450.8 ± 40.9	0.001**	0.091	0.224	0.001**

PLA, projected lung area; ΔPLA, difference of PLA between end-inspiration and end-expiration.
* stands for P value ≤ 0.050.
** stands for P value ≤ 0.010.
† P values are for the comparison of all groups by one-way analysis of variance.
‡ P values are for the comparison between Normal and COPD Mild groups.
§ P values are for the comparison between COPD Mild and Severe groups.
‖ P values are for the comparison between Normal and COPD Severe groups.

Table 3a
Spearman's correlation coefficients of PLA/ΔPLA with demographic data and PFTs in tidal respiration.

	tidal inspiration		tidal expiration		tidal ΔPLA	
Variables	r_s (95 %CI)	P value	r_s (95 %CI)	P value	r_s (95 %CI)	P value
Age	0.13 (-0.11, 0.35)	0.279	0.09 (-0.15, 0.31)	0.456	0.22 (-0.01, 0.43)	0.0498*
Sex	0.59 (0.42, 0.72)	<0.001**	0.56 (0.38, 0.70)	0.001**	0.24 (0.01, 0.45)	0.033*
Height	0.62 (0.46, 0.75)	<0.001**	0.64 (0.48, 0.76)	<0.001**	0.02 (-0.21, 0.25)	0.871
Weight	0.09 (-0.14, 0.32)	0.401	0.08 (-0.15, 0.31)	0.470	0.01 (-0.22, 0.24)	0.954
BMI	−0.31 (-0.51, −0.09)	0.006**	−0.35 (-0.54, −0.13)	0.002**	0.05 (-0.18, 0.28)	0.673
TV	0.20 (-0.03, 0.41)	0.084	0.17 (-0.07, 0.38)	0.145	0.24 (0.01, 0.45)	0.034*
VC	0.25 (0.02, 0.45)	0.031*	0.28 (0.05, 0.48)	0.014*	−0.09 (-0.32, 0.14)	0.415
%VC	−0.20 (-0.41, 0.03)	0.082	−0.15 (-0.37, 0.09)	0.203	−0.25 (-0.45, −0.02)	0.030*
FEV_1	−0.15 (-0.37, 0.08)	0.190	−0.07 (-0.30, 0.16)	0.533	−0.45 (-0.62, −0.24)	<0.001**
FEV_1%VC	−0.40 (-0.58, −0.19)	<0.001**	−0.33 (-0.52, −0.10)	0.004**	−0.50 (-0.62, −0.30)	<0.001**
%FEV_1	−0.42 (-0.60, −0.21)	<0.001**	−0.34 (-0.53, −0.12)	0.003**	−0.52 (-0.67, −0.33)	<0.001**

r_s means the Spearman's rank correlation coefficient.
BMI, body mass index; FEV_1, forced expiratory volume in one second; FEV_1%VC, forced expiratory volume percent in one second divided by forced vital capacity; %FEV_1, percent predicted forced expiratory volume percent in one second; %VC, percent predicted vital capacity; PFT, pulmonary functional test; PLA, projected lung area; ΔPLA, difference of PLA between end-inspiration and end-expiration; VC, vital capacity; TV, tidal volume.
* stands for P value ≤ 0.050.
** stands for P value ≤ 0.010.

Table 3b
Spearman's correlation coefficients of PLA/ΔPLA with demographic data and PFTs in forced respiration.

	forced inspiration		forced expiration		forced ΔPLA	
Variables	r_s (95 %CI)	P value	r_s (95 %CI)	P value	r_s (95 %CI)	P value
Age	0.06 (-0.17, 0.29)	0.586	0.01 (-0.22, 0.24)	0.924	0.02 (-0.21, 0.25)	0.836
Sex	0.65 (0.49, 0.77)	<0.001**	0.44 (0.23, 0.61)	<0.001**	0.36 (0.15, 0.55)	0.001**
Height	0.76 (0.64, 0.84)	<0.001**	0.48 (0.28, 0.64)	<0.001**	0.52 (0.33, 0.67)	<0.001**
Weight	0.25 (0.02, 0.45)	0.030*	−0.03 (-0.26, 0.20)	0.762	0.45 (0.25, 0.62)	<0.001**
BMI	−0.22 (-0.43, 0.01)	0.059	−0.38 (-0.56, −0.16)	<0.001**	0.21 (-0.02, 0.42)	0.061
TV	0.24 (0.01, 0.45)	0.036*	0.09 (-0.14, 0.31)	0.436	0.24 (0.01, 0.45)	0.032*
VC	0.43 (0.22, 0.60)	<0.001**	0.13 (-0.10, 0.35)	0.248	0.58 (0.40, 0.71)	<0.001**
%VC	−0.09 (-0.31, 0.15)	0.452	−0.28 (-0.48, −0.05)	0.014*	0.42 (0.22, 0.59)	<0.001**
FEV_1	0.02 (-0.21, 0.25)	0.857	−0.11 (-0.33, 0.12)	0.329	0.33 (0.11, 0.52)	0.003**
FEV_1%VC	−0.31 (-0.50, −0.08)	0.007**	−0.25 (-0.46, −0.02)	0.026*	−0.07 (-0.30, 0.16)	0.528
%FEV_1	−0.31 (-0.51, −0.09)	0.006**	−0.32 (-0.52, −0.09)	0.005**	0.002 (-0.23, 0.23)	0.986

r_s means the Spearman's rank correlation coefficient.
BMI, body mass index; FEV_1, forced expiratory volume in one second; FEV_1%VC, forced expiratory volume percent in one second divided by forced vital capacity; %FEV_1, percent predicted forced expiratory volume percent in one second; %VC, percent predicted vital capacity; PFT, pulmonary functional test; PLA, projected lung area; ΔPLA, difference of PLA between end-inspiration and end-expiration; VC, vital capacity; TV, tidal volume.
* stands for P value ≤ 0.050.
** stands for P value ≤ 0.010.

Table 4
Spearman's correlation coefficients of slope/intercept with demographic data and PFTs.

	slope		intercept	
Variables	r_s (95 %CI)	P value	r_s (95 %CI)	P value
Age	−0.03 (-0.26, 0.20)	0.768	0.17 (-0.07, 0.38)	0.149
Sex	0.10 (-0.13, 0.33)	0.364	0.66 (0.51, 0.77)	<0.001**
Height	0.24 (0.01, 0.45)	0.035*	0.72 (0.59, 0.81)	<0.001**
Weight	0.431 (0.20, 0.59)	<0.001**	0.23 (0, 0.44)	0.044*
BMI	0.38 (0.17, 0.56)	<0.001**	−0.20 (-0.41, 0.03)	0.076
TV	0.23 (0.001, 0.44)	0.043*	0.27 (0.05, 0.48)	0.014*
VC	0.46 (0.25, 0.623)	<0.001**	0.39 (0.18, 0.57)	<0.001**
%VC	0.38 (0.17, 0.656	<0.001**	−0.09 (-0.31, 0.15)	0.457
FEV_1	0.35 (0.13, 0.54)	0.002**	−0.05 (-0.28, 0.18)	0.637
FEV_1% VC	0.13 (-0.10, 0.35)	0.244	−0.39 (-0.57, −0.17)	<0.001**
%FEV_1	0.22 (-0.01, 0.43)	0.052	−0.36 (-0.55, −0.14)	0.001**

r_s means the Spearman's rank correlation coefficient.
BMI, body mass index; FEV_1, forced expiratory volume in one second; FEV_1%VC, forced expiratory volume percent in one second divided by forced vital capacity; %FEV_1, percent predicted forced expiratory volume percent in one second; %VC, percent predicted vital capacity; PFT, pulmonary functional test; VC, vital capacity; TV, tidal volume.
* stands for P value ≤ 0.050.
** stands for P value ≤ 0.010.

Several studies have reported the quantification of hyperinflation using chest CT volumetry [15,16]. However, supine positioning examination with the ignorance of gravity effect cannot perfectly reflect the physiological condition of COPD patients. The standing position during examination affected the better association between CT volumetry and total lung capacity in healthy volunteer group [17]. Schlesinger et al [18] presented that the estimation of total lung capacity from chest radiograph, which was mentioned in previous studies [19,20], had good correlation with actual total lung capacity, as well as that from chest CT. These previous studies may put greater importance on the standing position during examination.

With world-wide pandemic with coronavirus disease 2019, PFTs have a new challenge of requirement of contact via mouth piece with the testing system. The measurement system inevitably and potentially generates the artificial modification toward inspiratory and expiratory physiology due to the intrinsic resistance of the system. Patients can receive DXR with the mask on and without the touch of mouth, which can be the advantage toward ordinary pulmonary functional test.

DXR has another advantage toward PFTs. DXR can provide parameter of bilateral lung fields separately. Whereas, the results of unilateral lung cannot be obtained with PFTs.

Previous study in healthy volunteers showed the good correlation of PLA with pulmonary function; the estimation of pulmonary function by PLA was possibly suggested [12]. Accordingly, it is natural that ΔPLA in forced breathing showed the good and significant correlation with VC ($r_s = 0.58$; $p < 0.001$). This result indicates the possible use of DXR based PLA with automated tracking as an alternative method of the spirometry. Higher temporal resolution of DXR might have improved the correlation. On the other hand, ΔPLA in tidal breathing showed mild correlation with TV probably due to the failure to reflect inflation of lungs in ventrodorsal direction. It is also unignorable that ΔPLA in tidal respiration is smaller in Normal group than in COPD groups. No significant correlation was observed between %FEV_1 and PLA/ΔPLA in the previous study about healthy volunteers. Subtle hyperinflation of lungs in tidal respiratory phase of COPD patients could be well captured by DXR.

At the same time, we have to consider that ΔPLA can be affected by the precision of the measurement of PLA. Bland-Altman plot between manually and automatically tracked PLA suggested both fixed and proportional error though ICC was regarded as "almost perfect" agreement. DXR plays an important role in identifying particular respiratory phase for more precise measurement. However, there may be some room for improvement of automatic tracking method.

This study also showed the association of %FEV_1 with both PLA in each phase and intercept, probably suggesting that PLA quantified the degree of inflation of lungs. However, no studies have reported the quantification of hyperinflation of lungs with X-ray images. Ricieri et al [21] showed the association of chest diameter ratio with hyperinflation using photogrammetry of both transverse and sagittal views, while our study applied DXR images of only posteroanterior view. DXR is a simpler method with lower exposure dose than CT or fluoroscopy. DXR also provides physiological respiration in standing position, while CT or MRI examination is usually performed in supine position.

This study has several limitations. First, the number of cases is small, especially in COPD mild group. Further studies with large population are required to evaluate the reproducibility of this study. Second, DXR examinations is performed in only one department. The possibility cannot be denied that the obtained images are influence by radiologic technologists there. Third, the effect of the structure outside thorax is not considered in this study. The participants have the different degree of gastric gas below left diaphragm and the different level or shape of diaphragm. There is also a possibility that stiffness of neck and shoulder,

including slope shoulder or square shoulder, can lead to underestimation or overestimation of PLA. Fourth, the influence of the different condition of DXR is not assessed. COPD patients underwent DXR of tidal and forced breathing as a separate examination. Whereas healthy volunteers did that as a sequence of tidal breathing before forced breathing. These differences can affect the measured values of PLA. Fifth, contouring PLA was performed by one radiologist. Reproducibility between radiologist and automated tracking was evaluated only in forced inspiration. Sixth, Segmentation quality was not assessed in this study.

In conclusion, COPD patients had larger PLA than healthy volunteers in both lungs, indicating hyperinflation of lungs. Mild to moderate correlation was observed between PLA and $\%FEV_1$ as well as between ΔPLA in forced breathing and VC. Automated tracking of PLA is considered efficient for analysis.

Declaration of Competing Interest

The authors declare that they have no known competing financial interests or personal relationships that could have appeared to influence the work reported in this paper.

Appendix A. Supplementary material

Supplementary data to this article can be found online at https://doi.org/10.1016/j.ejrad.2022.110546.

References

[1] M. Decramer, W. Janssens, M. Miravitlles, Chronic obstructive pulmonary disease, Lancet 379 (2012) 1341–1351, https://doi.org/10.1016/S0140-6736(11)60968-9.

[2] D. Singh, N. Roche, D. Halpin, A. Agusti, J.A. Wedzicha, F.J. Martinez, Current controversies in the pharmacological treatment of chronic obstructive pulmonary disease, Am. J. Respir. Crit. Care Med. 194 (2016) 541–549, https://doi.org/10.1164/rccm.201606-1179PP.

[3] Global Initiative for Chronic Obstructive Lung Disease, Global strategy for the diagnosis, management, and prevention of chronic obstructive pulmonary disease 2021 report. https://goldcopd.org/2021-gold-reports, 2003 (accessed 12 January 2022).

[4] A. Jaitovich, E. Barreiro, Skeletal muscle dysfunction in chronic obstructive pulmonary disease. What we know and can do for our patients, Am. J. Respir. Crit. Care Med. 198 (2) (2018) 175–186.

[5] A. Rossi, Z. Aisanov, S. Avdeev, G. Di Maria, C.F. Donner, J.L. Izquierdo, N. Roche, T. Similowski, H. Watz, H. Worth, M. Miravitlles, Mechanisms, assessment and therapeutic implications of lung hyperinflation in COPD, Respir. Med. 109 (2015) 785–802, https://doi.org/10.1016/j.rmed.2015.03.010.

[6] C.B. Cooper, The connection between chronic obstructive pulmonary disease symptoms and hyperinflation and its impact on exercise and function, Am J Med 119 (2006) 21–31, https://doi.org/10.1016/j.amjmed.2006.08.004.

[7] N.R. Anthonisen, J.E. Connett, P.L. Enright, J. Manfreda, Lung Health Study Research Group, Hospitalizations and mortality in the Lung Health Study, Am. J. Respir. Crit. Care Med. 166 (2002) 333–339, https://doi.org/10.1164/rccm.2110093.

[8] R. Tanaka, S. Sanada, M. Suzuki, T. Kobayashi, T. Matsui, H. Inoue, N. Yoshihisa, Breathing chest radiography using a dynamic flat-panel detector combined with computer analysis, Med. Phys. 31 (2004) 2254–2262, https://doi.org/10.1118/1.1769351.

[9] A. Hata, Y. Yamada, R. Tanaka, M. Nishino, T. Hida, T. Hino, M. Ueyama, M. Yanagawa, T. Kamitani, A. Kurosaki, S. Sanada, M. Jinzaki, K. Ishigami, N. Tomiyama, H. Honda, S. Kudoh, H. Hatabu, Dynamic Chest X-Ray Using a Flat-Panel Detector System: Technique and Applications, Korean J. Radiol. 22 (2021) 634–651, https://doi.org/10.3348/kjr.2020.1136.

[10] T. Hida, Y. Yamada, M. Ueyama, T. Araki, M. Nishino, A. Kurosaki, M. Jinzaki, H. Honda, H. Hatabu, S. Kudoh, Decreased and slower diaphragmatic motion during forced breathing in severe COPD patients: Time-resolved quantitative analysis using dynamic chest radiography with a flat panel detector system, Eur. J. Radiol. 112 (2019) 28–36, https://doi.org/10.1016/j.ejrad.2018.12.023.

[11] Y. Yamada, M. Ueyama, T. Abe, T. Araki, T. Abe, M. Nishino, M. Jinzaki, H. Hatabu, S. Kudoh, Difference in diaphragmatic motion during tidal breathing in a standing position between COPD patients and normal subjects: Time-resolved quantitative evaluation using dynamic chest radiography with flat panel detector system ("dynamic X-ray phrenicography), Eur. J. Radiol. 87 (2017) 76–82, https://doi.org/10.1016/j.ejrad.2016.12.014.

[12] T. Hino, A. Hata, T. Hida, Y. Yamada, M. Ueyama, T. Araki, T. Kamitani, M. Nishino, A. Kurosaki, M. Jinzaki, K. Ishigami, H. Honda, H. Hatabu, S. Kudoh, Projected lung areas using dynamic X-ray (DXR), Eur J Radiol Open. 7 (2020), 100263, https://doi.org/10.1016/j.ejro.2020.100263.

[13] B.L. Graham, I. Steenbruggen, M.R. Miller, I.Z. Barjaktarevic, B.G. Cooper, G. L. Hall, T.S. Hallstrand, D.A. Kaminsky, K. McCarthy, M.C. McCormack, C. E. Oropez, M. Rosenfeld, S. Stanojevic, M.P. Swanney, B.R. Thompson, Standardization of spirometry 2019 update. An official American Thoracic Society and European Respiratory Society technical statement, Am. J. Respir. Crit. Care Med. 200 (8) (2019) e70–e88.

[14] Y. Kanda, Investigation of the freely available easy-to-use software 'EZR' for medical statistics, Bone Marrow Transplant 48 (2013) 452–458, https://doi.org/10.1038/bmt.2012.244.

[15] G.R.T. Alves, E. Marchiori, K.L. Irion, P.J.Z. Teixeira, D.C. Berton, A.S. Rubin, B. Hochhegger, The effects of dynamic hyperinflation on CT emphysema measurements in patients with COPD, Eur. J. Radiol. 83 (2014) 2255–2259, https://doi.org/10.1016/j.ejrad.2014.08.014.

[16] M. Shen, E.D. Tenda, W. McNulty, J. Garner, H. Robbie, V. Luzzi, A. M. Aboelhassan, W.H. Van Geffen, S.V. Kemp, C. Ridge, A. Devaraj, P.L. Shah, G. Z. Yang, Quantitative evaluation of lobar pulmonary function of emphysema patients with endobronchial coils, Respiration 98 (2019) 70–81, https://doi.org/10.1159/000499622.

[17] Y. Yamada, M. Yamada, S. Chubachi, Y. Yokoyama, S. Matsuoka, A. Tanabe, Y. Niijima, M. Murata, K. Fukunaga, M. Jinzaki, Comparison of inspiratory and expiratory lung and lobe volumes among supine, standing, and sitting positions using conventional and upright CT, Sci. Rep. 10 (2020) 16203, https://doi.org/10.1038/s41598-020-73240-8.

[18] A.E. Schlesinger, D.K. White, G.B. Mallory, C.F. Hildeboldt, C.B. Huddleston, Estimation of total lung capacity from chest radiography and chest CT in children: Comparison with body plethysmography, Am. J. Roentgenol. 165 (1995) 151–154, https://doi.org/10.2214/ajr.165.1.7785574.

[19] H.M. Loyd, S.T. String, A.B. DuBois, Radiographic and plethysmographic determination of total lung capacity, Radiology 86 (1995) 7–14, https://doi.org/10.1148/86.1.7.

[20] P.C. Pratt, G.A. Klugh, A method for the determination of total lung capacity from posteroanterior and lateral chest roentgenograms, Am. Rev. Respir. Dis. 96 (1967) 548–552, https://doi.org/10.1164/arrd.1967.96.3.548.

[21] D.d.V. Ricieri, N.A. Rosário, J.R. Costa, Chest diameter ratios for detecting static hyperinflation in children using photogrammetry, J. Pediatr. 84 (5) (2008) 410–415.